

Assignment

Homework HW1

Enrico Dalla Mora - 10937966

Michele Murciano - 10883559

Musical Acoustics



POLITECNICO
MILANO 1863

October 22, 2023

Characterization of a string instrument soundboard

Finite element method appendix

The finite element method consists in an approximate but very general formulation that can be applied to develop the numerical model of any kind of structure. It is based on the idea of dividing the structure in a certain number of small portions called **finite elements**. This is achieved by a particular space discretization in the space dimensions, which is implemented by the construction of a mesh of the object. In each element some remarkable points called *nodes* are identified and their displacement is described by a set of nodal coordinates. The motion of any other point inside the element is then expressed as a function of the nodal coordinates through proper shape functions. The systematic nature of **FEM** makes it general and widely employable in different fields of study.

a) Soundboard design

- Geometry

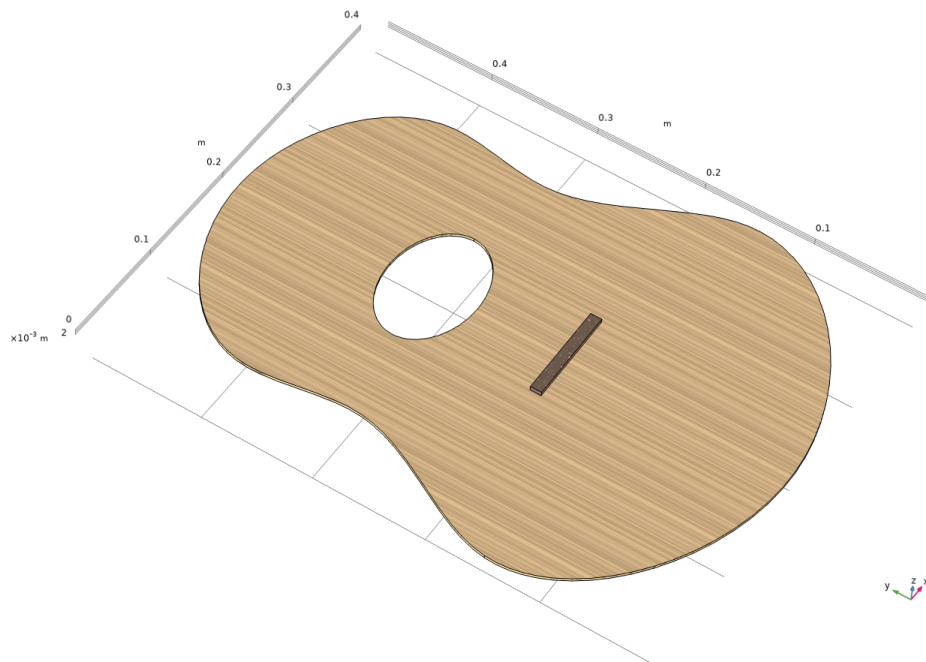


Figure 1: Geometry of the designed soundboard and bridge.

The designed soundboard emulates the one of a guitar with an elliptical sound hole. Shape and dimensions approximate the one of a real guitar but are not that precise since these details go beyond the scope of interest of this study. The 3D component is obtained by extruding the correspondent 2D components for the soundboard and the bridge in opposite z directions. The 2D soundboard shape is achieved by designing two ellipses which have been interpolated. Finally a third ellipse is subtracted from the 2D geometry in order to create the sound hole. The bridge, on the other hand, is extruded from a simple rectangle. The thickness of the soundboard is set to **2.5 mm** while the one of the bridge is set to **4 mm**. The other main dimensions of the plate are **40 x 50 cm**. As a last step useless edges or vertices must be removed before meshing.

- Mesh

The mesh is obtained by employing different meshing techniques for different domains. In particular a free tetrahedral mesh with extremely fine dimension forms the bridge. The soundboard instead is formed by a swept of the top surface's triangular mesh with a distribution of 5 elements along the thickness of the board. Note that, as a result of the process employed, the bottom surface will present as the top one a distribution affected by the presence of the bridge. This way the two surfaces match allowing the swept to be computed. The mesh statistics for the whole and final mesh report an average element quality of 0.8606 (on a scale from 0 to 1) which has to be considered as acceptable.

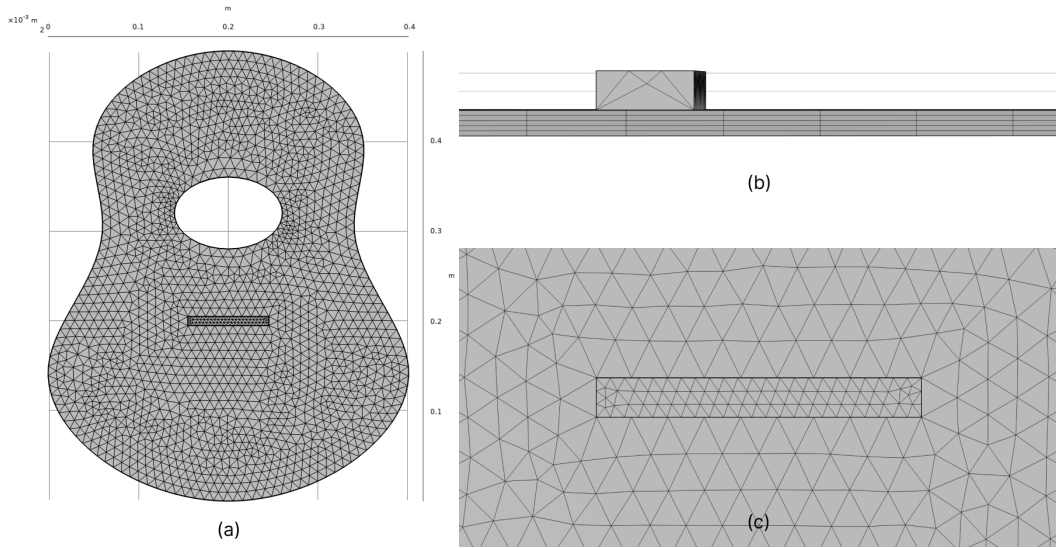


Figure 2: Object meshing → (a) front view, (b) swept distribution detail from side view, (c) tetrahedral bridge meshing detail.

- Materials

For the purposes of the study different materials must be defined.

- Isotropic Engelmann spruce for the whole structure.
- Orthotropic version of the Engelmann spruce for the whole structure.
- Orthotropic Red Maple for the bridge combined with orthotropic Engelmann Spruce for the soundboard.

The values for *density*, *Young's moduli*, *shear moduli* and *Poisson's ratios* which define the materials properties are reported in the table below:

| Density [kg/m ³] | | | |
|------------------------------|------------|------------|------------|
| Engelmann Spruce | | | 350 |
| Red Maple | | | 540 |
| Young's Moduli [GPa] | | | |
| | E_L | E_R | E_T |
| Engelmann Spruce | 9.79 | 1.25 | 0.58 |
| Red Maple | 12.43 | 1.74 | 0.83 |
| Shear Moduli [GPa] | | | |
| | G_{LR} | G_{RT} | G_{LT} |
| Engelmann Spruce | 1.21 | 0.10 | 1.17 |
| Red Maple | 1.65 | 0.30 | 0.92 |
| Poissons's Ratios | | | |
| | ν_{LR} | ν_{RT} | ν_{LT} |
| Engelmann Spruce | 0.422 | 0.53 | 0.462 |
| Red Maple | 0.434 | 0.762 | 0.509 |

Figure 3: Materials specifications.

- Physics

Finally, as a last step before beginning the computation of the various studies, a physics interface must be defined as to specify the physical field of interest and the rules governing it. For this purpose the *solid mechanics* interface has to be employed. This component will govern the specific boundary conditions, loads and the material type employed.

b) Eigenfrequency study in free boundary (isotropic spruce)

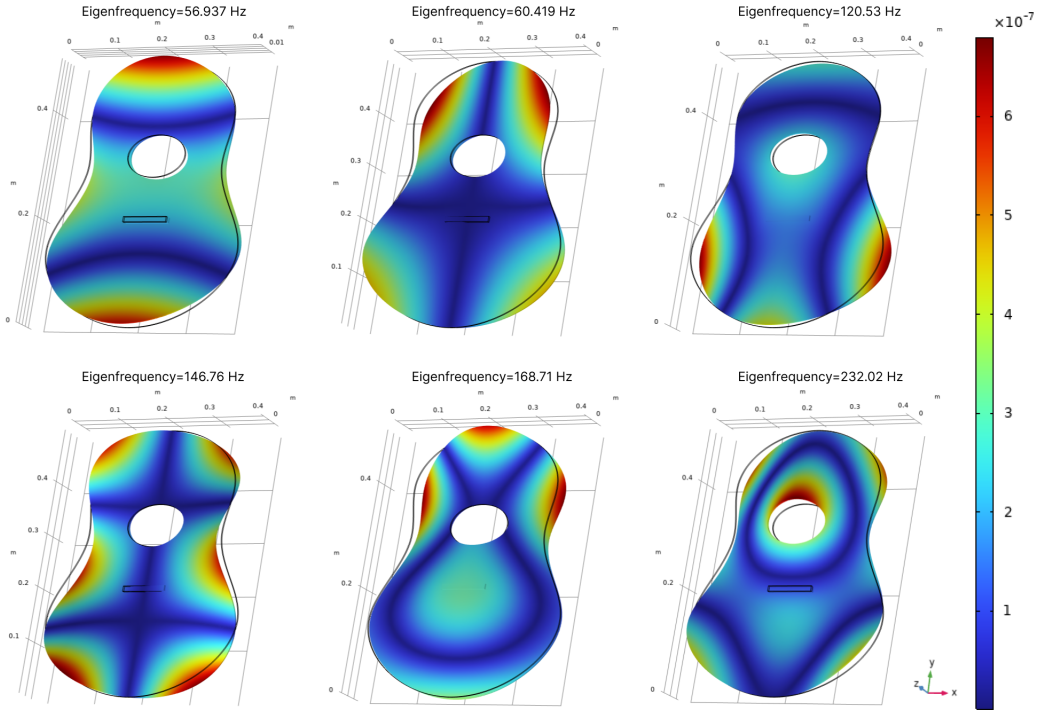


Figure 4: First six modes in free boundary condition (isotropic material).

In this section the modes for the correspondent eigenfrequencies of the board in free boundary condition are evaluated in the case of isotropic Engelmann spruce. The results are computed for the first twenty eigenfrequencies even though only the first six are reported in figure (4). Note that the first values computed by the eigenfrequencies study are negligible because they are related to numerical errors or to rotational/translational motion of the plate in free boundary. It can be noticed that the first mode at 56.937 Hz resembles an *x-mode*. The reason why the modeshape differs from the ideal *x-mode* relies on the fact that, for isotropic materials, the *x-mode* and *ring-mode* manifest only if the plate is square shaped as can be seen in figure (5). It will be seen in section 4 and 5 that, for an orthotropic material, this condition is no longer valid. Instead, the aspect ratio for which these modes can be seen will depend on the Young moduli of the material.

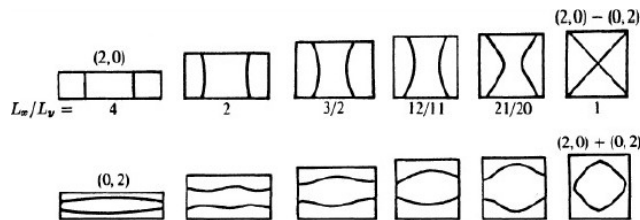


Figure 5: X and ring modes for varying aspect ratios in a rectangular plate.

In the same way, modes 3, 5 and 6 somehow resemble *ring modes*. It is also clear that the second mode resembles the (1,1) mode of an equivalent rectangular plate and the same goes for the fourth mode which can be associated to the mode (1,2).

c) Eigenfrequency study with fixed constraints (isotropic spruce)

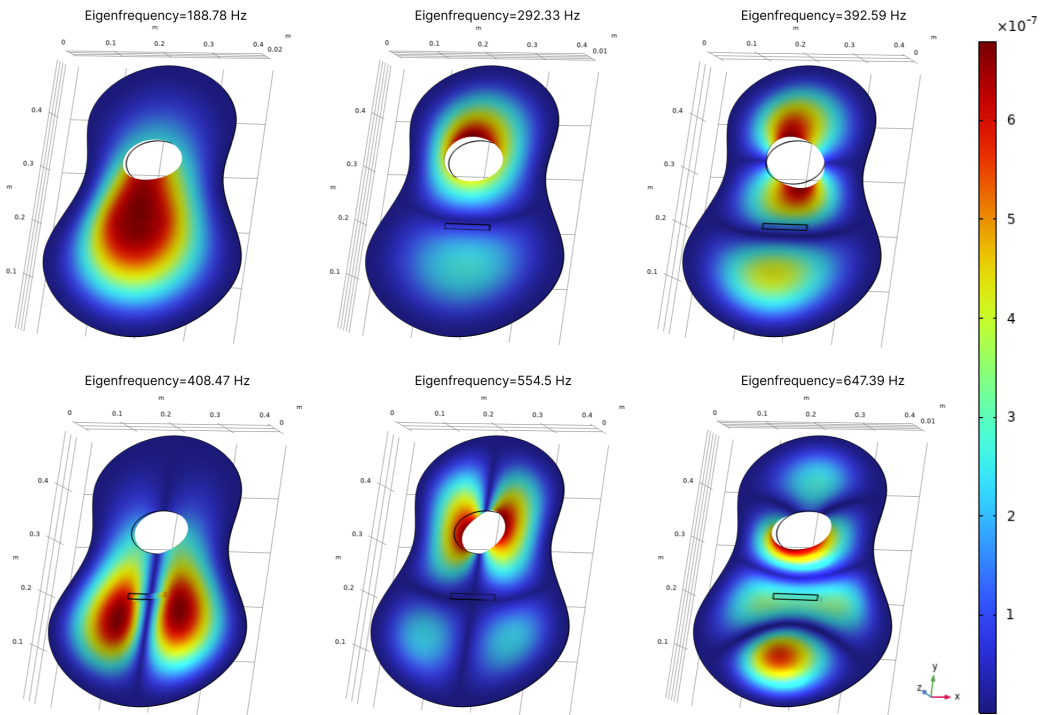


Figure 6: First six modes with fixed constraints to the sides (isotropic material).

Now, the same modeshapes and eigenfrequencies are computed in the case of fixed sides (displacement $z(t) = 0$). This is perfectly coherent with the graphs in which the displacement of areas close to the sides of the plate is very small or even null. As before, the complexity of the vibrating modes increases with frequency and it is easy to identify nodal lines. Evaluating vibrational modes w.r.t. the ones of a vibrating rectangular plate, it is possible to establish a parallelism identifying the m and n modal indexes of an equivalent rectangular plate. In particular these indexes, from the first mode to the sixth one, will respectively be (0,0), (0,1), (0,2), (1,0), (1,1), (0,3).

d) Eigenfrequency study in free boundary (orthotropic spruce)

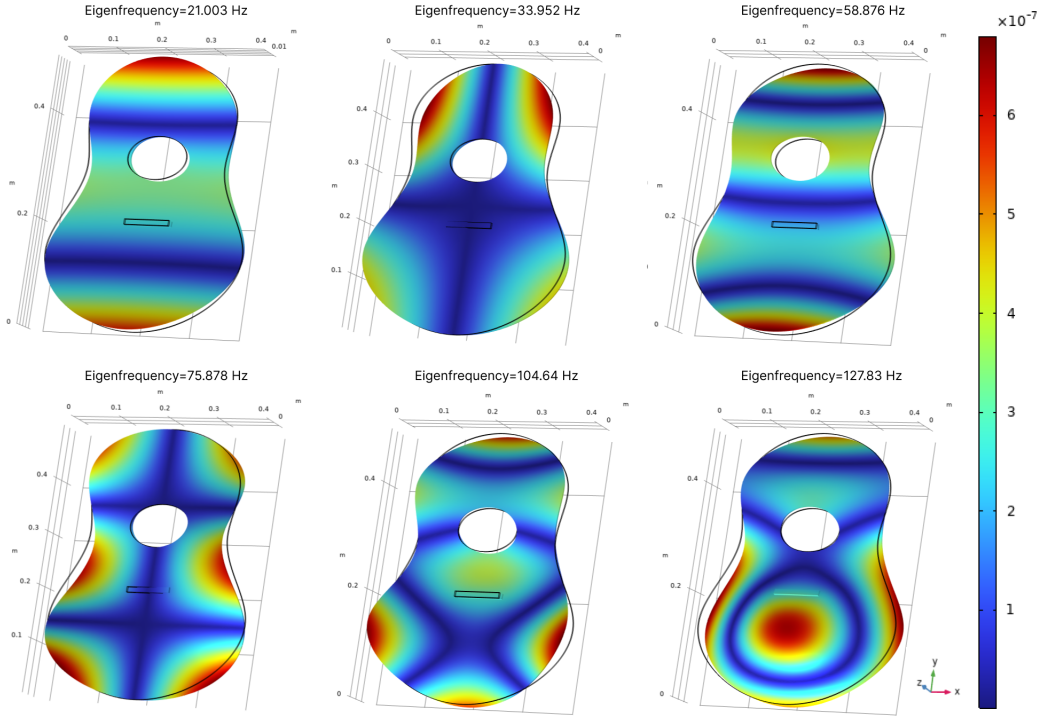


Figure 7: First six modes in free boundary condition (orthotropic material).

By changing the material to an orthotropic one and repeating the same study conducted in section 2 these modeshapes are obtained. The similarity with figure (4) is clear, but it's important to notice how eigenfrequencies changed. As an effect of lowering the Young moduli in non-longitudinal directions, lower frequencies w.r.t. the isotropic version are obtained for the correspondent mode shape. It is also important to point out that, in the case of orthotropic material, *x* and *ring* modes can be obtained for a rectangular thin plate with aspect ratio defined by the following relation:

$$\frac{L_L}{L_R} = \left(\frac{E_L}{E_R}\right)^{\frac{1}{4}} \quad (1)$$

In the case of a non-rectangular thin plate it is possible to approximate this value by evaluating the average length of the plate. Given this analysis, it is still not easy to identify these particular mode shapes with the specific conditions of this study.

e) Eigenfrequency study with fixed constraints (orthotropic spruce)

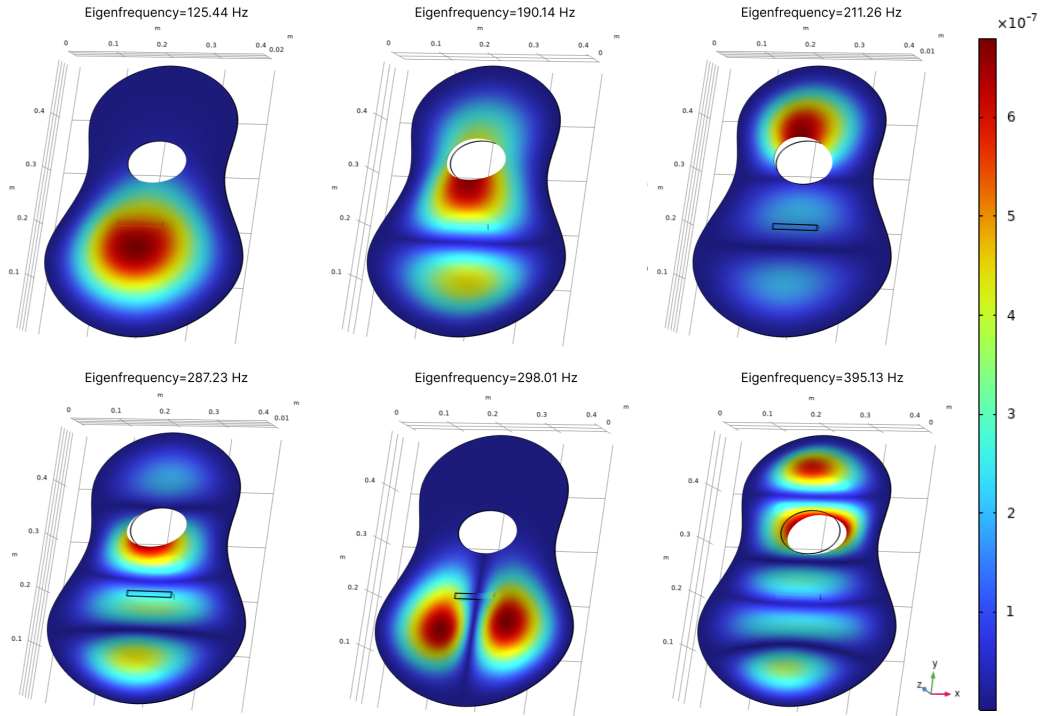
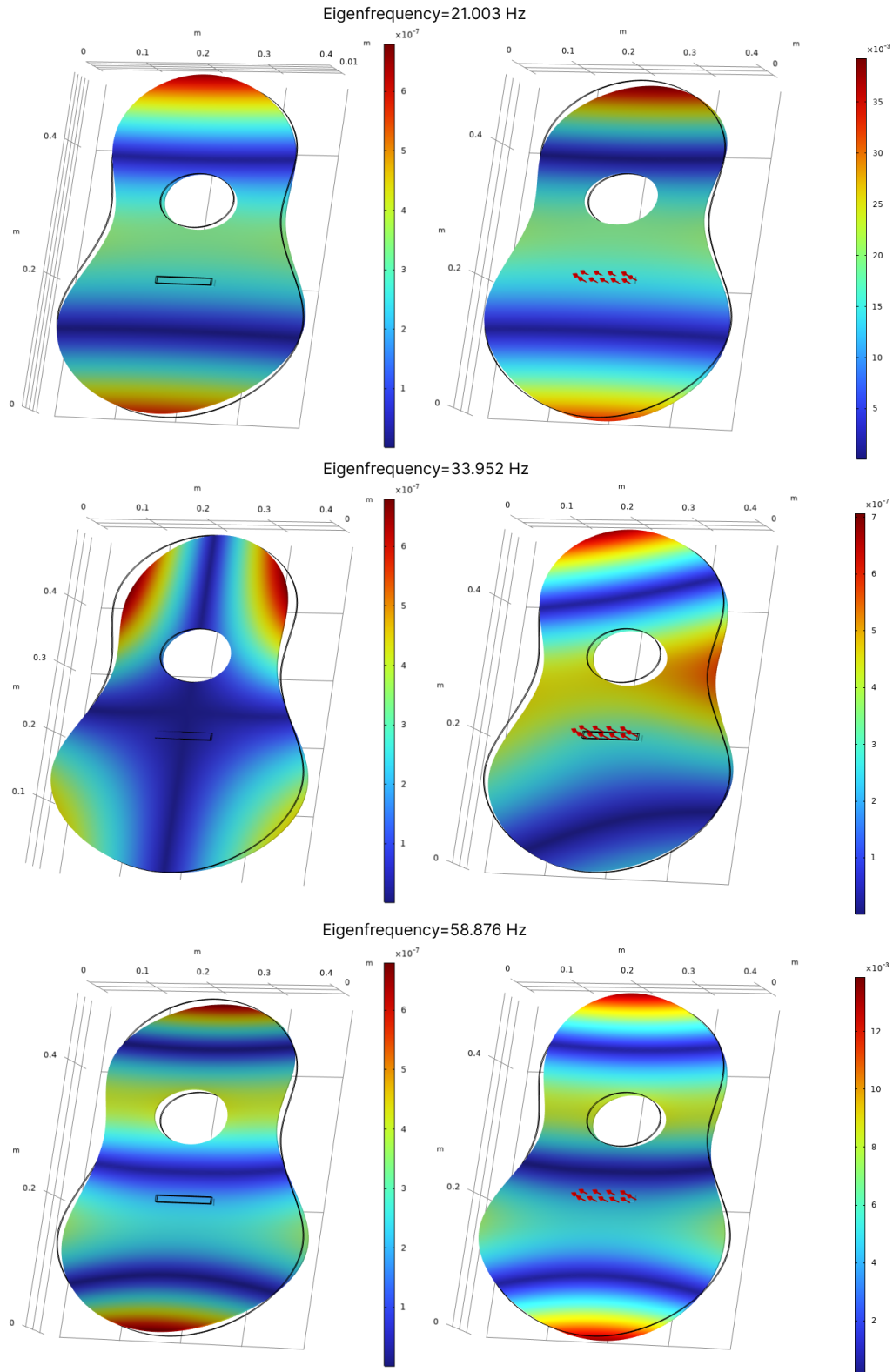


Figure 8: First six modes with fixed constraints to the sides (orthotropic material).

The same goes for the fixed edges modal analysis with the new material. As before, lowering the Young moduli in the non-longitudinal directions will result in lower resonance frequencies.

f) Frequency domain simulation in free boundary with surface load

Let's now evaluate the response of the soundboard to an harmonic force of varying frequency applied to the bridge's surface. In this case the bridge is built of orthotropic Red Maple while the soundboard remains of Engelmann Spruce. The results are computed for frequencies in range 10–500 Hz with a step of 5 Hz. The specific response for eigenfrequencies of the first five modes are also calculated in order to quantify the effect of resonances. In the following graph the results are reported for the first five eigenfrequencies, the other values computed will be useful in the evaluation of the mobility at the bridge contact area (section 7).



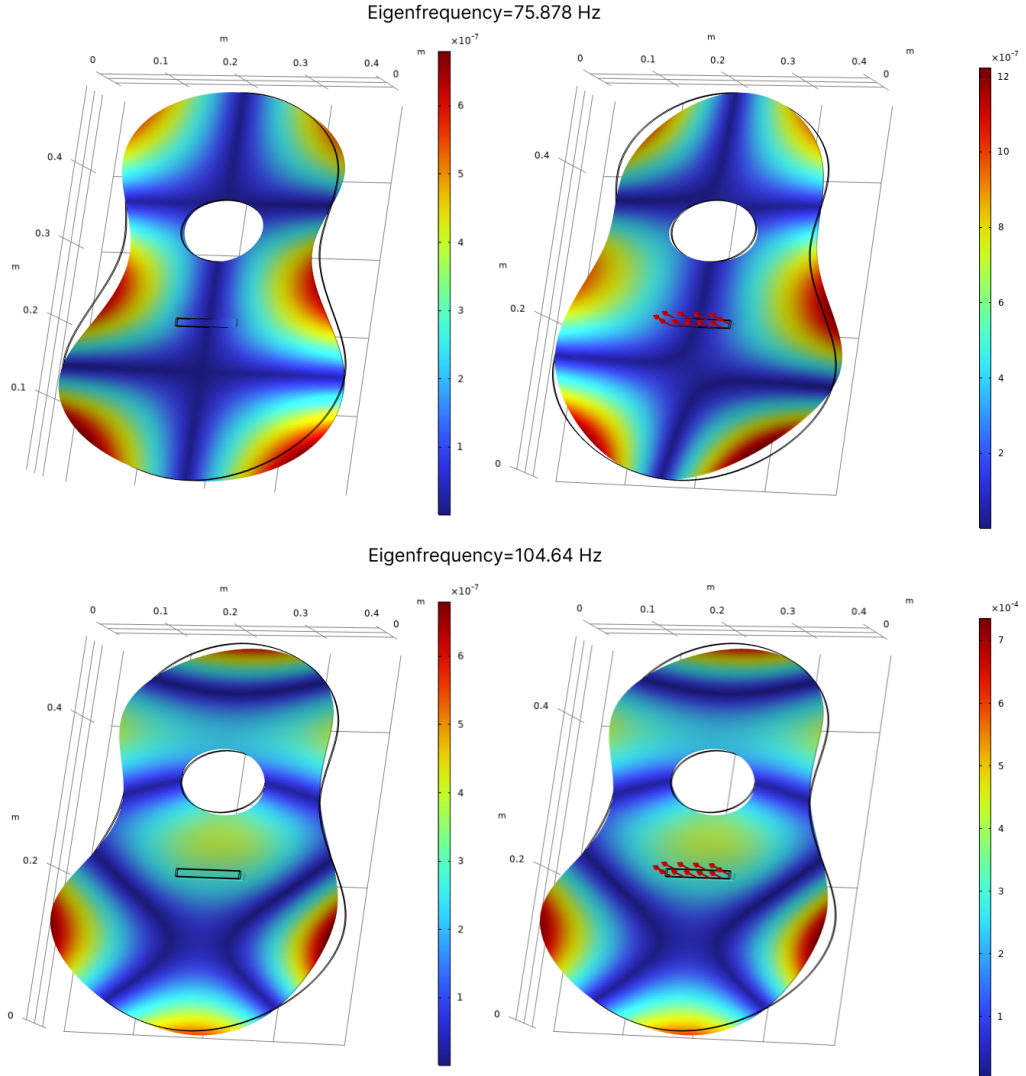


Figure 9: On the left: Free boundary eigenfrequency simulation, on the right: plate response to an harmonic load applied on the bridge surface at that frequency.

First of all, it's important to notice how modal shapes manifest when the excitation force resonates with the natural frequencies of the system. This is clear by the similarity between the responses and the mode shapes themselves. Moreover, by looking at the scale of the response it is possible to see how the second and fourth modes (33.95 and 75.87 Hz) resonate with a much lower magnitude than the others. This is caused by the fact that, for those particular modes, the excitation point coincides with nodal lines. This phenomenon will also be highlighted in figure (10) where resonance peaks in correspondence of those frequencies won't manifest.

g) Bridge average velocity

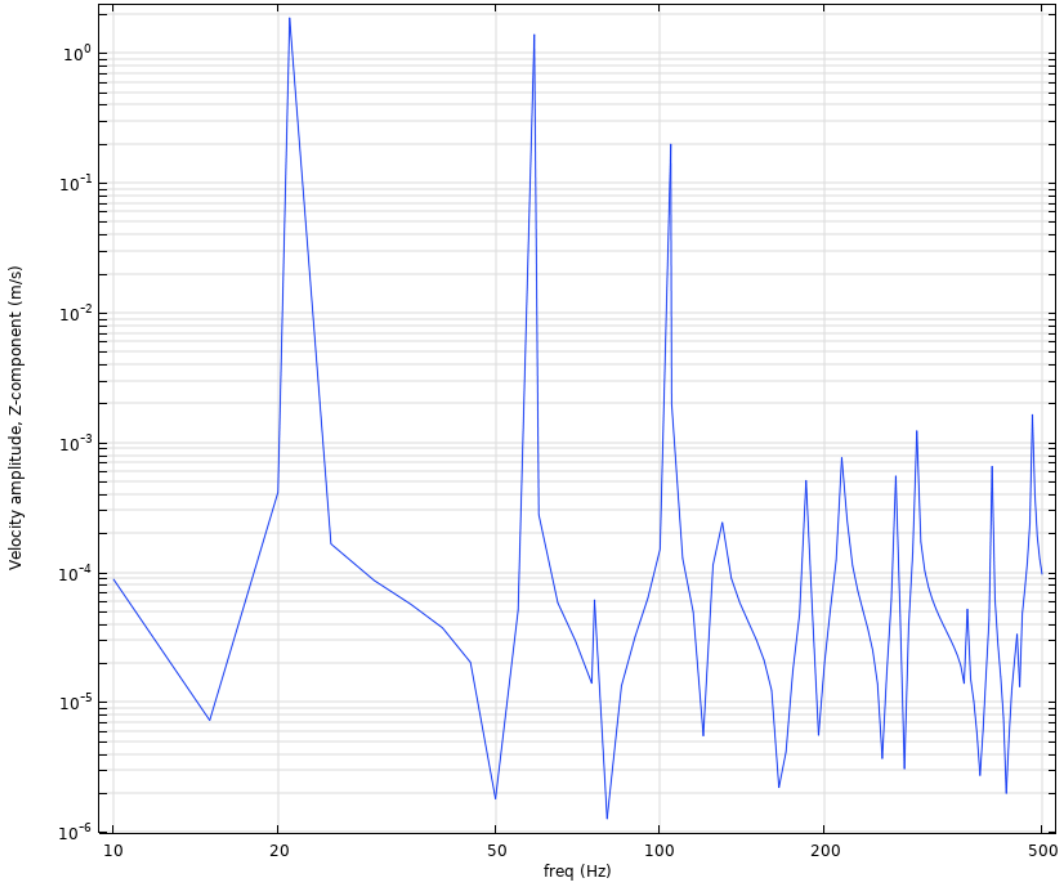


Figure 10: Average velocity in the z-direction on the bridge's surface.

As a last step, the z-component of the average of the velocity field over the contact area between the bridge and soundboard is computed for the frequency range defined in the previous study. As before said, resonances are evident for the first, third and fifth mode, while for the second and fourth modes the magnitude of the velocity is relatively small as an effect of the excitation point coinciding with nodal lines. Finally, figure (10) can be regarded as a mobility frequency response function, being the magnitude of the excitation force equal to 1 N/m. This being said, logarithmic scales has been adopted both for x and y axis in order to achieve a better representation.